Cerebral Cortex, November 2017;27: 5156–5169

doi: 10.1093/cercor/bhw297
Advance Access Publication Date: 3 October 2016
Original Article

ORIGINAL ARTICLE

Altered Global Signal Topography in Schizophrenia

Genevieve J. Yang[1,2,3], John D. Murray[1], Matthew Glasser[4], Godfrey D. Pearlson[1,5], John H. Krystal[1,2,6], Charlie Schleifer[1], Grega Repovs[7], and Alan Anticevic[1,2,3,5,6,8]

[1]Department of Psychiatry, Yale University School of Medicine, 300 George Street, New Haven, CT 06511, USA, [2]Department of Neuroscience, Yale University School of Medicine, 333 Cedar Street, New Haven, CT 06520, USA, [3]Abraham Ribicoff Research Facilities, Connecticut Mental Health Center, New Haven, CT 06519, USA, [4]Department of Neurobiology, Washington University School of Medicine, Saint Louis, MO, USA, [5]Olin Neuropsychiatry Research Center, Institute of Living, Hartford Hospital, 200 Retreat Avenue, Hartford, CT 06106, USA, [6]NIAAA Center for the Translational Neuroscience of Alcoholism, New Haven, CT 06519, USA, [7]Department of Psychology, University of Ljubljana, Ljubljana, Slovenia, and [8]Department of Psychology, Yale University, 2 Hillhouse Avenue, New Haven, CT 06520, USA

Address correspondence to Alan Anticevic, Yale University, Department of Psychiatry, 34 Park St., New Haven, CT 06519, USA.
Email: alan.anticevic@yale.edu

Abstract

Schizophrenia (SCZ) is a disabling neuropsychiatric disease associated with disruptions across distributed neural systems. Resting-state functional magnetic resonance imaging has identified extensive abnormalities in the blood-oxygen level-dependent signal in SCZ patients, including alterations in the average signal over the brain—i.e. the "global" signal (GS). It remains unknown, however, if these "global" alterations occur pervasively or follow a spatially preferential pattern. This study presents the first network-by-network quantification of GS topography in healthy subjects and SCZ patients. We observed a nonuniform GS contribution in healthy comparison subjects, whereby sensory areas exhibited the largest GS component. In SCZ patients, we identified preferential GS representation increases across association regions, while sensory regions showed preferential reductions. GS representation in sensory versus association cortices was strongly anti-correlated in healthy subjects. This anti-correlated relationship was markedly reduced in SCZ. Such shifts in GS topography may underlie profound alterations in neural information flow in SCZ, informing development of pharmacotherapies.

Key words: association cortex, default mode network, frontoparietal control network, resting state, sensory cortex

Introduction

Schizophrenia (SCZ) is a severe mental illness associated with abnormal belief formation, hallucinations (Kay et al. 1987), and anhedonia (Berenbaum and Oltmanns 1992). The illness co-occurs with neuronal disturbances affecting diverse cortical regions: primary visual (Lencz et al. 2003; Calderone et al. 2013) and auditory circuits (Javitt et al. 1997; Vercammen et al. 2010; Hoffman et al. 2011), as well as association regions linked to higher-order cognitive deficits (Goldman-Rakic 1994; Tek et al. 2002; Stephan, Friston et al. 2009). Consistent with these diverse clinical and neural effects, pharmacological models of SCZ often propose a distributed disruption in excitation/inhibition (E/I) ratio across the cortex, such as is suggested by the *N*-methyl-D-aspartate receptor hypo-function hypothesis (Krystal et al. 2003; Jardri and Deneve 2013; Schobel et al. 2013). This hypothesis is supported by clinical magnetic resonance spectroscopy studies showing GABA (gamma-aminobutyric acid) and glutamate deficits across cortex in SCZ

(Marsman et al. 2013; Marsman et al. 2014; Poels et al. 2014; Taylor and Tso 2015). Further evidence suggests that some areas may be preferentially affected by hypothesized widespread E/I elevations in SCZ. In particular, the prefrontal cortex (PFC) plays a central role in executive processing (Cole et al. 2014) and working memory (Goldman-Rakic 1994)—both considered core cognitive deficits in SCZ (Barch and Ceaser 2012). Converging neuroimaging findings implicate preferential disturbances in PFC and other association regions in SCZ (Whitfield-Gabrieli et al. 2009; Baker et al. 2014; Yang et al. 2014; Gupta et al. 2015; Radhu et al. 2015; Yang et al. 2016), with corresponding thalamo-cortical dysconnectivity (Woodward et al. 2012; Anticevic et al. 2014). Additional postmortem evidence from SCZ studies shows disrupted gene expression (Akbarian et al. 1996; Dracheva et al. 2001; Hashimoto et al. 2003, 2008; Maldonado-Aviles et al. 2009) and localized reductions in dendritic spine density (Glantz and Lewis 2000), which may impact synaptic mechanisms regulating signaling in association cortices.

Critically, these macro-scale disruptions in brain system function can be studied using noninvasive neuroimaging, which is increasingly applied to understand psychiatric illness (Johnson et al. 2006; Welsh et al. 2010; Woodward et al. 2012; Anticevic et al. 2014). Specifically, functional magnetic resonance imaging (fMRI) studies have captured differences between the blood-oxygen level-dependent (BOLD) signal in SCZ patients and healthy comparison subjects (HCS), suggesting altered brain activity during particular mental tasks (task-based state, tb), as well as in the absence of tasks (resting-state, rs) (Lowe 2012). Yet, major methodological barriers remain for developing parsimonious and neurobiologically grounded interpretations of rs-fMRI effects. Specifically, rs-fMRI studies have revealed altered BOLD signal fluctuations, indicating that gray matter signals are more temporally variable in SCZ relative to HCS (Yang et al. 2014), a finding that is especially prominent in association cortices (Yang et al. 2014, 2016). Such spatially specific elevations in cortical BOLD variance may represent a basic functional disruption in SCZ, which requires consideration when interpreting functional connectivity findings. Simply put, locally altered BOLD variability may impact functional connectivity estimates, for example, correlations computed between regions, which are inherently normalized by local BOLD variability. This consideration is further complicated by the use of global signal (GS) regression, a common pre-processing step for rs-fMRI (Fox et al. 2009).

In brief, the GS is defined as the spatial average of time-varying BOLD signals across the brain. This signal has been hypothesized to reflect non-neuronal sources of noise, such as head motion or physiological artifacts (Power et al. 2014), which can spuriously impact brain-wide BOLD signal. Thus, GS is often removed, along with other "nuisance" signals, which results in more spatially specific functional network definitions (Fox et al. 2009). However, use of GS regression (GSR) can be controversial (Saad et al. 2012), especially in between-group clinical comparisons wherein the GS may itself contain clinically meaningful information (Yang et al. 2014). That is, GS likely contains both neuronal (Schölvinck et al. 2010) and non-neuronal signals, and the former may provide important clues to healthy neurobiology as well as neuropathological processes in clinical conditions.

The GS will, by definition, share some resemblance to any gray matter BOLD signal. However, the degree to which a specific brain region's BOLD signal resembles the GS (i.e. its statistical relationship to the GS) will not necessarily be identical across regions. Interestingly, the spatial mapping of GS representation across the brain has been under-studied in the literature. The first reported whole-brain map of GS topography in healthy subjects (Aguirre et al. 1997; Zarahn et al. 1997) was generated to establish that voxels across the brain overwhelmingly show positive correlation with the GS. Since this first report, few studies have pursued detailed analyses of GS topography and no studies have formally quantified its potential shifts in SCZ, leaving vital knowledge gaps regarding our understanding of this widely used, yet controversial, analytic step. Here, we present the first network-by-network analysis of GS topography in healthy subjects, as well as comparisons with GS topography in SCZ. Critically, we hypothesized that GS topography would dissociate across sensory and association networks in healthy subjects on average. We generated this hypothesis because sensory cortices are thought to primarily process external incoming stimuli, which strongly drive "bottom-up" processing across parallel circuits and networks. In this way, sensory stimulation potentially "entrains" cortical processing and leads to higher levels of correlated activity throughout sensory networks, which may lead to a stronger GS contribution. Put simply, these highly correlated sensory signals will not cancel each other out with averaging. In contrast, higher-order association cortices need to represent multiple information streams and maintain distinct representations independently over time, perhaps resulting in less shared activity across association areas. Consequently, association signals will statistically tend to cancel out with averaging, producing a relatively weaker contribution to the GS. Thus, different computational roles of sensory versus association cortex may contribute to their distinct GS representation pattern in healthy subjects.

In turn, we predicted significant GS topography shifts in SCZ. Prior work revealed that SCZ is associated with elevations in cortical BOLD signal variance relative to HCS (Yang et al. 2014). This group difference was significantly attenuated by GSR, suggesting that variance effects in SCZ may reflect concurrent changes in their GS. Yet, no study has formally examined if GS changes in SCZ occur homogenously across the brain or arise from specific regional disruptions. Put differently, while existing findings suggest abnormal GS in SCZ, implicating a global disturbance, it is currently unknown whether the severity of this disturbance may differ across regions or follow a homogenous brain-wide pattern. Given existing evidence for network preferential alterations in SCZ (Woodward et al. 2012; Anticevic et al. 2014; Baker et al. 2014; Yang et al. 2016), we hypothesized that BOLD signals in SCZ might also show network-dependent changes in their statistical relationship to the GS.

Materials and Methods

Participants

We studied two independent clinical samples that were combined for the purposes of the present analysis (Table S1). One sample comprised 90 chronic SCZ patients and 90 demographically matched HCS recruited at the Olin Neuropsychiatry Research Center through outpatient clinics and community mental health facilities in the Hartford. The second sample, comprised of 71 SCZ and 74 demographically matched HCS, was obtained from a publicly distributed dataset provided by the Center for Biomedical Research Excellence (COBRE) (http://fcon_1000.projects.nitrc.org/indi/retro/cobre.html). All participants provided informed consent approved by the institutional review board of relevant institutions. Across samples, all subjects met identical neuroimaging exclusion criteria, underwent

identical preprocessing and analyses. SCZ symptom severity, across both samples, was determined using the Positive and Negative Syndrome Scale (PANSS) (Kay et al. 1987) (Table S1).

Inclusion & Exclusion Criteria

Patients were included based on the following criteria: (1) SCZ diagnosis as determined by the Structured Clinical Interview (SCID) for the Diagnostic and Statistical Manual of Mental Disorders-IV (First et al. 2002), administered by experienced MA or PhD-level research clinicians; (2) no major medical or neurological conditions (e.g. epilepsy, migraine, head trauma with loss of consciousness); and (3) premorbid IQ > 70 as assessed by National Adult Reading Test, Wide Range Achievement Test or Wechsler Test of Adult Reading depending on the study protocol (Spreen and Strauss 1998). As in prior studies, these measures were normed and converted to IQ equivalents for each subject. If more than one premorbid achievement measure was available per subject the scaled scores were averaged per standard practice (Lezak 1995). To increase ecological validity of the patient sample (Krystal et al. 2006), comorbid Axis I anxiety disorders and/or history of substance abuse (fully remitted >6 months before the study) were allowed. HCS participants were excluded if they had: (1) history of medical or neurological disorders, (2) history of mental retardation, (3) history of severe head trauma with >5 min loss of consciousness; (4) history of substance abuse or dependence within the last 12 months, (5) current or lifetime Axis I psychiatric disorder as assessed by SCID-NP; (6) history of psychotic disorders in first-degree relatives (reported by detailed family history). Across samples we accomplished matching on a number of relevant demographic variables. Patients and HCS did not significantly differ on any of the variables (see Table S1), apart from educational attainment and premorbid intellectual functioning (IQ), which were lower for SCZ. These differences are impacted by the illness course (Glahn et al. 2006) (43) and thus were not included as a covariate. All medication was converted to chlorpromazine equivalents (Andreasen et al. 2010) and verified by trained raters. Notably, smoking status and medication dose did not alter reported effects (see Figure S4 for comprehensive confound analyses).

Neuroimaging Data Acquisition

At the Olin Neuropsychiatry Research Center 90 SCZ and 90 HCS were scanned using a Siemens-Allegra 3 T scanner with identical acquisition parameters (Anticevic, Brumbaugh et al. 2012). Images sensitive to BOLD signal were acquired with axial slices parallel to the anterior-posterior commissure (AC-PC) using a T2*-weighted gradient-echo, echo-planar sequence (TR/TE = 1500/27 ms, flip angle = 60°, field of view = 24 × 24 cm, acquisition matrix = 64 × 64, voxel size = 3.43 × 3.43 × 4 mm). The acquisition lasted 5.25 min and produced 210 volumetric images per subject (29 slices/volume, inter-slice gap = 1 mm). Subjects were instructed to lay awake in the scanner and keep their eyes open. Subjects were monitored on a video camera to ensure that they stayed awake and were removed from the analyses if they fell asleep during the scan or if their head movement exceeded 1 mm along any axis. Structural images were acquired using a T1-weighted, 3D magnetization-prepared rapid gradient-echo (MPRAGE) sequence (TR/TE/TI = 2200/4.13/766 ms, flip angle = 13°, voxel size [isotropic] = 0.8 mm, image size = 240 × 320 × 208 voxels), with axial slices parallel to the AC-PC line.

As noted, 71 additional SCZ patients and 74 matched HCS underwent data collection at COBRE using a Siemens Tim-Trio 3 T scanner. Full acquisition details are reported previously (Stephan, Penny et al. 2009; Hanlon et al. 2011; Mayer et al. 2012). Briefly, BOLD signal was collected with 32 axial slices parallel to the AC-PC using a T2*-weighted gradient-echo, echo-planar sequence (TR/TE = 2000/29 ms, flip angle = 75°, acquisition matrix = 64 × 64, voxel size = 3 × 3 × 4 mm). The acquisition lasted 5 min and produced 150 volumetric images per subject. Structural images were acquired using a 6-minute T1-weighted, 3D MPRAGE sequence (TR/TE/TI = 2530/[1.64, 3.5, 5.36, 7.22, 9.08]/900, flip angle = 7°, voxel size [isotropic] = 1 mm, image size = 256 × 256 × 176 voxels), with axial slices parallel to the AC-PC line. Described parameters were obtained via the website (http://fcon_1000.projects.nitrc.org/indi/retro/cobre.html).

Neuroimaging Preprocessing

Preprocessing followed prior work (Cole et al. 2011; Anticevic, Brumbaugh et al. 2012); complete fMRI acquisition and preprocessing details are presented in Supplement together with some limitations to these legacy acquisition and preprocessing methods. Notably, as part of standard preprocessing, we used multiple regression to model the time-varying BOLD signal in each voxel, including a nuisance regressor for the mean signal across gray matter aka the GS (as well as other typical nuisance regressors, e.g. for white matter, ventricular signal, and rigid body motion). This step was performed after the data were scrubbed for high motion (see Supplementary Material). From this multiple regression, we obtained beta weights for each regressor variable. Presented analyses concern the voxel-wise beta weights obtained for the nce regressor for the mean signal across GS, assessed in SCZ and HCS.

Global Gray Matter Signal Beta Map Calculation

To obtain GS beta values, we first performed GSR using standard widely adopted procedures (Cole et al. 2011; Anticevic, Brumbaugh et al. 2012). The GS timeseries for each subject was obtained by calculating mean raw BOLD signal averaged over all gray matter voxels for each time point, explicitly excluding ventricles and white matter signal (which are defined as separate nuisance regressors). This GS timeseries was used as nuisance predictor term within a multiple linear regression model along with other nuisance predictor terms (ventricular signal, white matter signal, movement parameters, and the first derivatives of each of these with respect to time). Critically, we did not use the first derivative of the GS as an additional nuisance regressor, as this would have produced 2 GS-related beta weights rather than one. We computed the multiple regression with a single GS-related variable to yield a more parsimonious interpretation of the obtained voxel-wise GS beta weight. More formally, we used the following multiple regression analysis:

$$\begin{aligned} \mathrm{BOLD}_k^{\mathrm{raw}}(t) &= b_0 + \textstyle\sum_{i=1}^{n} b_i X_i \; + \; \mathrm{BOLD}_k^{\mathrm{preprocessed}}(t) \\ &= b_0 + b_{\mathrm{GS}}\mathrm{GS}(t) \; + \; \textstyle\sum_{i=2}^{n-1} b_i X_i \; + \mathrm{BOLD}_k^{\mathrm{preprocessed}}(t), \end{aligned}$$

where $\mathrm{BOLD}_k^{\mathrm{raw}}(t)$ represents the raw BOLD signal in voxel k as a function of time, t. b_0 is the intercept, containing trend parameters for the scan, X_i represents the ith nuisance regressor (e.g. ventricles or GS), b_i is the corresponding beta weight computed for regressor X_i. The last term is the residual signal that is not accounted for by the nuisance regressors. In other words, the residual represents the preprocessed BOLD signal at voxel

k. As noted, the n nuisance regressors include GS(t), ventricular signal V(t), white matter signal WM(t), 6 movement parameters, and first derivatives of the latter 8 with respect to time. The GS beta weights reported are represented by the b_{GS} values obtained from this multiple regression. GS(t) is the spatial average of time-varying BOLD signal across all gray matter voxels:

$$GS(t) = \frac{\sum_k^m BOLD_k(t)}{m}$$

The "Mean GS beta weight" computation in Figures 1F, 2D–E, 3C–D, and 4 is done by simply fitting a generalized linear model (GLM) to each voxel's BOLD time series to obtain the GS beta weight (b_{GS}) as shown above, and then averaging across each voxel belonging to the region of interest. Importantly, the voxel-wise whole-brain map of GS beta weights is more akin to a task-based GLM analysis than to a functional connectivity measure. In other words, GS beta weights are not functional connectivity values and should not be interpreted as such.

Functional Network Definition

In addition to the voxel-wise regression analyses, we used an *a priori* functional network parcellation to explicitly quantify the presence (or absence) of GS beta spatial shifts in SCZ. For this purpose, we employed a preexisting functional parcellation computed by Power et al. (2011). We defined boundaries for the following higher-order association networks: default mode network (DMN), frontoparietal control network (FPCN), and ventral attention network (VAN). Similarly, we isolated the visual, auditory, and somatosensory networks. These network boundaries were used to provide independent validation of voxel-wise effects (Power et al. 2011).

Results

Defining Spatial Localization of the GS in Healthy Individuals

We first examined the spatial pattern of GS representation in healthy subjects. Of note, instead of computing voxel-wise correlations to the GS—as was done in earlier work (Aguirre et al. 1997; Zarahn et al. 1997; Fox et al. 2009), here we utilize beta coefficients obtained using multiple regression (see Exp. Procedures available in Supplementary Material). This measure of GS representation has some advantages when aiming to account for GS along with multiple nuisance regressors simultaneously. Critically, the GS component in a given voxel's BOLD signal is expressed as $b_{GS}GS(t)$, where the regressor variable GS(t) is a function of time, and the beta coefficient b_{GS} is spatially-varying across voxels (see Exp. Procedures available in Supplementary Material). We hypothesized that this proportion of GS (b_{GS}) at each voxel may show a distinct spatial pattern across the brain in healthy subjects. We quantified the beta coefficients, b_{GS}, across all gray matter voxels in a sample of 164 healthy subjects, producing a group-level T-map of voxel-wise GS beta values (Fig. 1A,B, see Table S2 for region coordinates and statistics surviving whole-brain type I error correction). We observed a strikingly nonuniform representation of GS across functional brain networks: b_{GS} values were significantly greater in sensory than in association network regions (Fig. 1 F) [$t(163) = 9$, paired samples test, $P < 4 \times 10^{-16}$]. To clarify, this analysis compared 2 measures (mean association and mean sensory region GS beta weight) within each subject and not between subjects: The voxel-wise GS beta weights were averaged across association and sensory regions within a given single subject first—iterating this process produced a pair of subject-specific values for each subject, using only data from

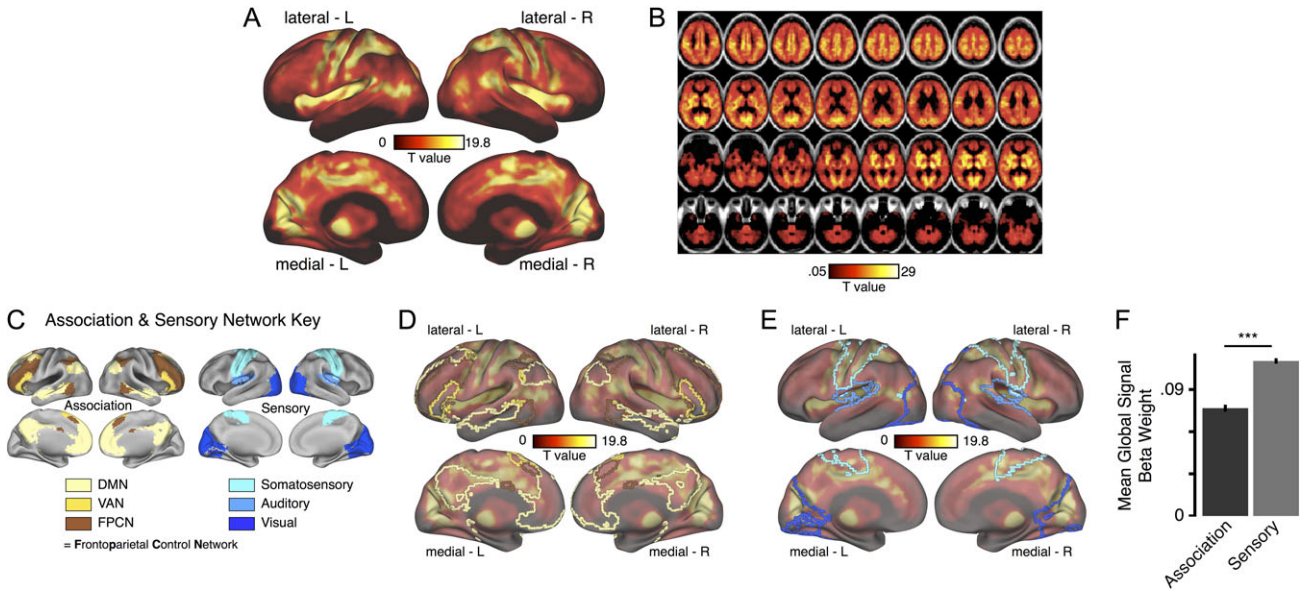

Figure 1 Mapping GS Topography in Healthy Individuals. (*A*) Surface visualization of type I error-protected group-level T-map computed across healthy subjects' (n = 164) whole-brain voxel-wise GS beta coefficient values, showing nonuniform distribution of GS beta weights. Note that the T-map highlights positive GS beta values and covers virtually the entire brain due to the statistical power obtained from examining 164 people. (*B*) Volume-based visualization of (*A*). (*C*) Resting-state functional network-based parcellations obtained from Power et al. (2011) were used to define areal boundaries for the association cortex (comprised of frontoparietal control network aka FPCN, default mode network aka DMN, and ventral attention network aka VAN), and the sensory cortex (comprised of somatosensory aka SS, auditory aka AUD, and visual aka VIS regions). (*D*) Same T-map as in (*A*), with borders of the 3 association networks (DMN, VAN, and FPCN) overlaid. (*E*) Same T-map as in (*A*), with borders of the 3 sensory networks (SS, AUD, and VIS) overlaid. (*F*) Using the ROIs defined in (*C*), we conducted an *a priori* analysis of mean GS beta weights in association versus sensory network regions in healthy subjects. Results show significantly higher GS beta weights in sensory compared with association networks, quantitatively supporting spatially nonuniform distribution of GS in healthy adults. ***$P < 0.001$.

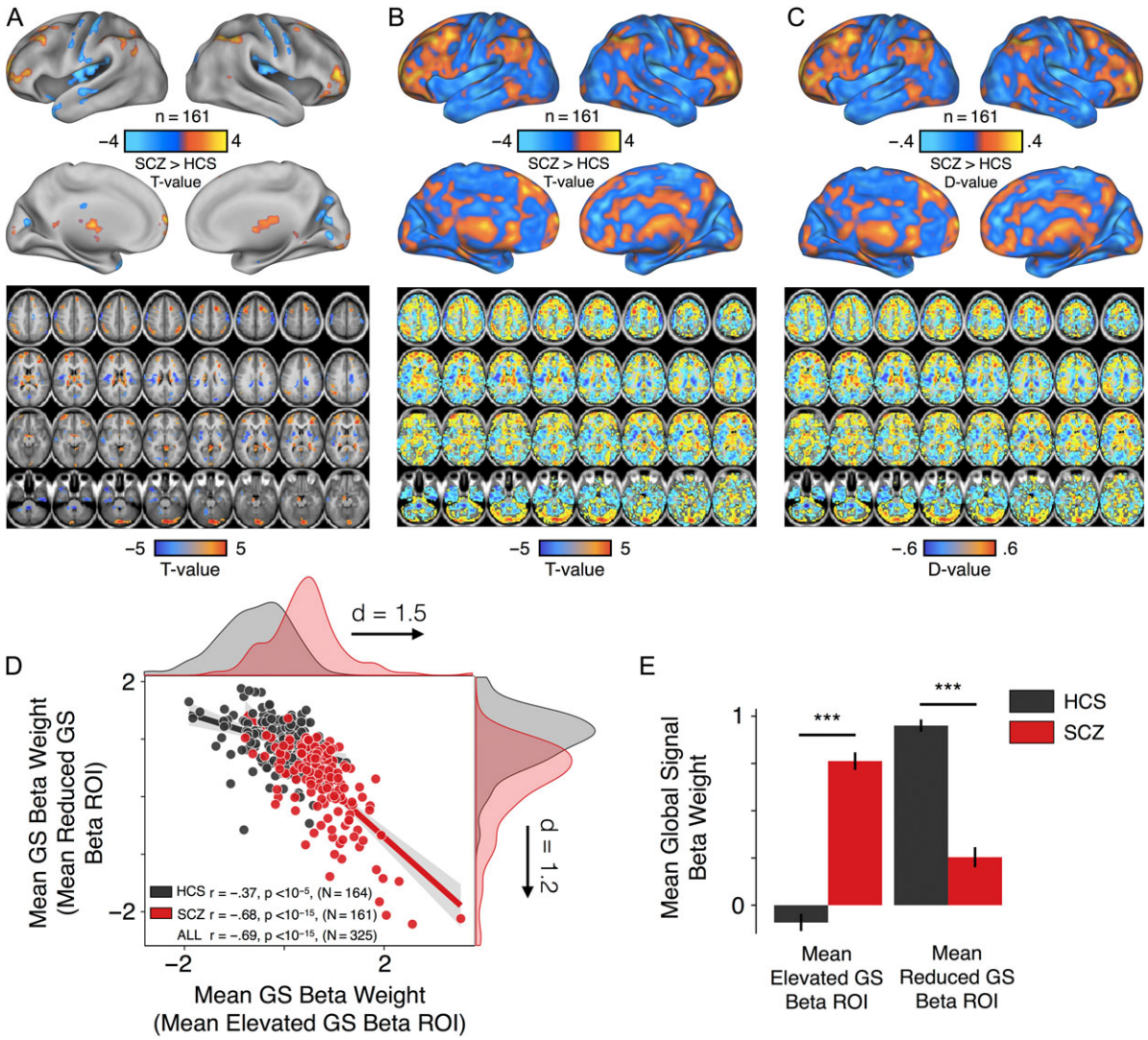

Figure 2. GS Representation is Spatially Altered in SCZ. (*A*) Type I error-protected voxel-wise surface and volumetric T-map comparing GS beta values for the full SCZ (n = 161) and HCS (n = 164) group. Sensory regions show reductions in GS representation, while association regions show increases in GS, for SCZ relative to HCS (see Table S3 for full list of regions; see Fig. 4 for network overlap calculation). These results combine 2 independent data samples collected from 2 different sites. Unthresholded results are shown in (*B*). (*C*) Cohen's d map of unthresholded results from (*B*) illustrating moderate-sized effects. Using the T-map from (*A*), we defined voxels of significantly increased GS representation in SCZ as the "Mean Elevated GS Beta" region, and voxels of significantly reduced GS representation in SCZ as the "Mean Reduced GS Beta" region. Averaging across voxels within these regions for each subject, we present the group distribution for each within-subject average GS beta weight value, for each region (*D*). We also report the Pearson correlation between dependent measures in the scatter plot. The red and black trend lines are regression lines from a fitted linear model of the data for SCZ and HCS, respectively, with shading representing the 95% confidence interval (CI) on the fitted values. d = Cohen's d effect size. (*E*) Bar plot representation of group mean values from (*D*), showing significant differences between groups. ***$P < 0.001$. Error bars represent standard error of the mean.

that subject. These subject-specific values for mean association and mean sensory GS beta weights were then compared for all healthy subjects in a paired samples t-test. Further, mean b_{GS} in sensory versus association networks exhibited a significant anti-correlation across healthy subjects—those with larger sensory b_{GS} had smaller association b_{GS} (Fig. 5C) [r = −0.37, $P < 10^{-6}$].

GS Representation is Spatially Altered in SCZ

Prior work showed that GS may be altered in SCZ relative to HCS (Yang et al. 2014). We hypothesized that the spatial pattern of GS representation may be altered in SCZ. To test this, we mapped b_{GS} values in SCZ, exactly as was done for the healthy subjects (Fig. 1 & S1). Then we computed a T-map comparing SCZ versus HCS groups to identify areas in SCZ that might be altered in their statistical relationship to the GS. Results revealed significant group differences in whole-brain voxel-wise b_{GS} values (Fig. 2), with distributed clusters of significant elevations and reductions in voxel-wise b_{GS} for SCZ (Fig. 2A, see Table S3 for region coordinates and statistics surviving whole-brain type I error correction). In addition, the unthresholded T-map (Fig. 2B) and Cohen's D map (Fig. 2C) show a pattern of b_{GS} increases and reductions that qualitatively co-localize to association versus sensory networks respectively (see quantitative analysis in Fig. 4). The whole-brain T-maps of GS beta weights for SCZ and HCS groups are separately shown in Figure S1.

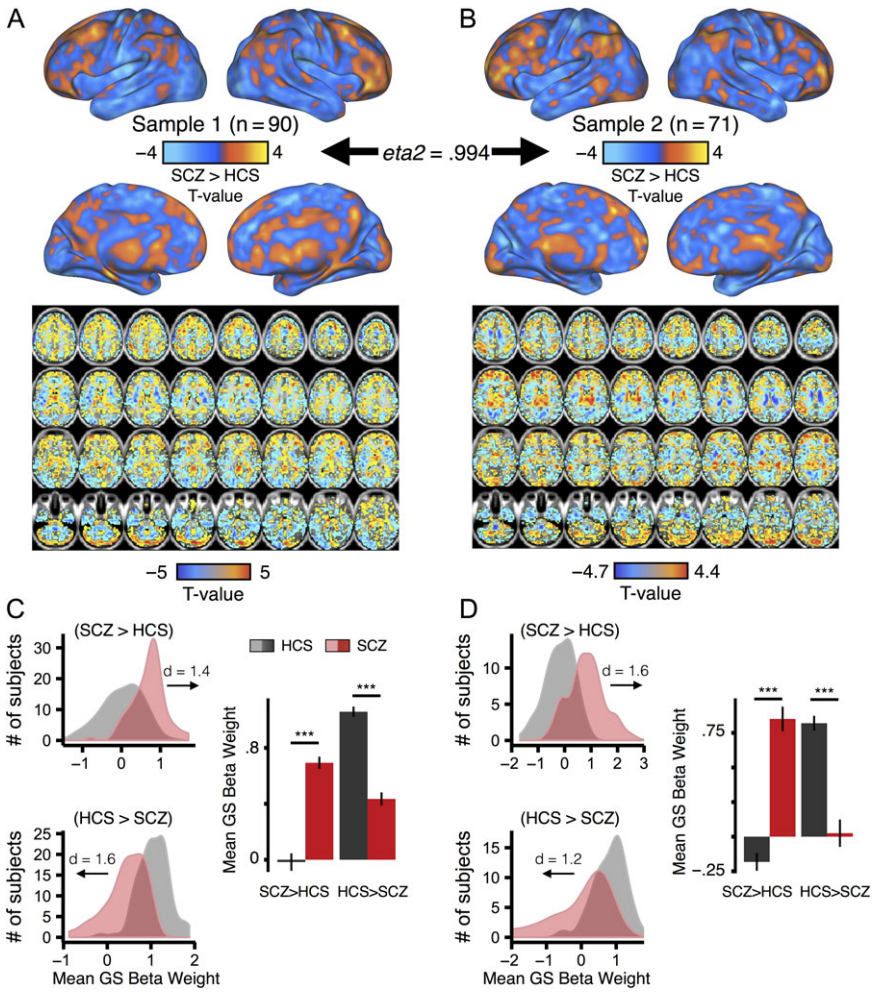

Figure 3. Qualitative Comparison of GS Shifts Across Clinical Samples. As mentioned, Figure 2A results combine 2 independent data samples collected from 2 different sites. Unthresholded T-map results for Sample 1 (from Yale) alone are shown in (A). Unthresholded results for Sample 2 (from Centers of Biomedical Research Excellence, COBRE) alone are shown in (B). Note while there are some minor qualitative differences, the statistical similarity between maps in panels A and B (Samples 1 & 2 respectively) was exceptionally high (eta^2 = 0.994 for the full range of T-values), indicating high correspondence of the spatial GS shifts in SCZ across independent samples. (C) Using the T-map from Figure 2A, we defined voxels of significantly increased GS representation in SCZ as the "SCZ > HCS" region (aka the "Mean Elevated GS Beta" ROI in Fig. 2), and voxels of significantly reduced GS representation in SCZ as the "HCS > SCZ" region (aka the "Mean Reduced GS Beta" ROI in Fig. 2). We present the Sample 1 group distributions and mean GS beta weight values for areas defined in Figure 2. (D) Results for Sample 2, computed as in (C). ***$P < 0.001$. d = Cohen's d effect size. Error bars represent standard error of the mean.

Notably, the overall sample was collected across 2 sites (Table S1). We observed a similar qualitative pattern of GS beta changes when examining unthresholded between-group maps separately for each sample (Fig. 3A,B). For the full sample, effects extracted from the type I error corrected ROIs quantitatively confirmed increases [$t(322) = 13$, $P < 3 \times 10^{-16}$, Cohen's $d = 1.5$] and reductions [$t(267) = 11$, $P < 3 \times 10^{-16}$, Cohen's $d = 1.2$] in SCZ relative to HCS (Fig. 2D,E). Finally, this bi-directional effect was quantified via a 2-way ANOVA analysis examining a "Group × ROI" interaction [$F(1,323) = 192.2$, $P < 2 \times 10^{-16}$]. In addition, these "Group" effects replicated when examining samples separately by site (Fig. 3C,D) for both the mean elevated GS beta ROI [$t(160) = 9$, $P < 3 \times 10^{-16}$, Cohen's $d = 1.4$ for Sample 1; $t(128) = 9$, $P < 3 \times 10^{-16}$, Cohen's $d = 1.6$ for Sample 2], and the mean reduced GS beta ROI [$t(168) = 10$, $P < 3 \times 10^{-16}$, Cohen's $d = 1.6$ for Sample 1; $t(108) = 7$, $p < 2 \times 10^{-10}$, Cohen's $d = 1.2$ for Sample 2]. Again, these effects were quantified via a 2-way ANOVA analysis examining a Group x ROI interaction [$F(1,178) = 121.8$, $P < 2 \times 10^{-16}$ for Sample 1; $F(1,143) = 87.3$, $P < 2 \times 10^{-16}$ for Sample 2].

In turn, we quantified the spatial similarity between the obtained T-maps for samples 1 & 2, using a measure of voxel-wise similarity (eta^2) (Cohen et al. 2008). The aim was to quantify the spatial reproducibility of the between-group differences in GS topography shifts (see SI Appendix for details). Figure 3 shows the quantified similarity index (eta^2 = 0.994 for full range of T-values), revealing a high degree of spatial reproducibility for the between-group GS topography differences across samples.

Next, we examined if altered GS localization increases and reductions in SCZ were quantitatively related. Using the T-map results shown in Figure 2A, we defined specific regions of significantly elevated b_{GS} in SCZ (the mean elevated GS beta ROI). Similarly, we defined regions of significant b_{GS} reductions in SCZ (the mean reduced GS beta ROI). We averaged voxel-wise b_{GS} values in each large ROI. Results indicated that b_{GS} values for the 2 sets of ROIs were negatively correlated for all groups

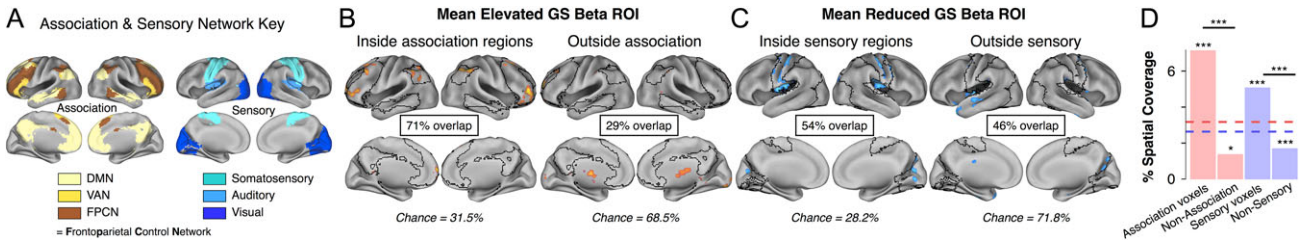

Figure 4. Quantifying Overlap Between Increased GS Localization in SCZ & Independently Defined Networks. (*A*) Using a priori defined, network-based parcellations, we defined areal boundaries for the association cortex (comprised of frontoparietal control network, default mode network, and ventral attention network), and the sensory cortex (comprised of somatosensory, auditory, and visual regions). (*B*) 71% of voxels showing significantly elevated GS representation in SCZ (Fig. 2A) overlapped with the association networks (31.5% of total gray matter voxels belong to association networks). In contrast, for the "outside association" region, defined as all cortical gray matter not belonging to the 3 presented association networks, there was far less overlap with regions of elevated GS representation (29%) than expected by chance (68.5%). (*C*) 54% of voxels showing significantly reduced GS representation in SCZ (Fig. 2A) overlapped with the sensory networks (28.2% of total gray matter voxels belong to sensory networks). In contrast, for the "outside sensory" region, defined as all cortical gray matter not belonging to the 3 presented sensory networks, there was far less overlap with regions of reduced GS representation (46%) than expected by chance (71.8%). (*D*) The significance above each bar represents the result from binomial tests computed for (*B*–*C*), comparing the expected percentage of significant voxels with the observed percentage of total significant voxels lying within each region. Binomial tests for the pink bars were computed on voxels showing significant elevations in GS representation in SCZ relative to HCS, assessing their overlap with the "inside association" and "outside association" regions. Binomial tests for the blue bars were computed on voxels showing significant reductions in GS representation in SCZ relative to HCS, assessing their overlap with "inside sensory" and "outside sensory" regions. The percent spatial coverage plotted represents the total number of significant voxels in a region, divided by the total number of voxels for that region. The significance between bars marks difference between proportions, comparing spatial coverage within association regions (or sensory regions) with spatial coverage outside. The red dashed line marks the spatial coverage of all gray matter voxels by voxels showing significantly increased GS representation; the blue dashed line marks the spatial coverage of all gray matter voxels by voxels showing significantly reduced GS representation (see Fig. 2A). ***$P < 0.001$, *denotes $P < 0.05$.

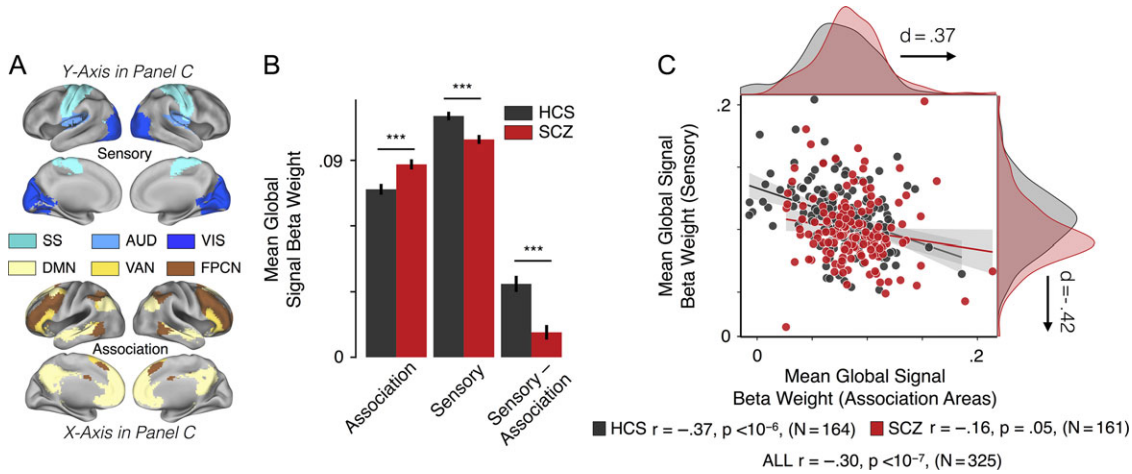

Figure 5. GS Representation in Association Regions is Negatively Correlated with GS Representation in Sensory Regions. (*A*) Using *a priori* defined, network-based parcellations, we extracted signal for the association cortex (comprised of frontoparietal control network aka FPCN, default mode network aka DMN, and ventral attention network aka VAN), and the sensory cortex (comprised of somatosensory aka SS, auditory aka AUD, and visual aka VIS regions). (*B*) Results from (*A*) represented in bar plot form, highlighting a significant difference of group means for both association and sensory region GS representation. The rightmost bars, "Sensory – Association", show the difference between mean sensory and mean association GS beta weights for each group. ***$P < 0.001$. Error bars represent +/–1 standard error of the mean for association and sensory beta weights, standard error of the difference of means for the "Sensory – Association" bars. (*C*) Mean voxel-wise GS beta weights in association regions and in sensory regions are plotted on the *x* and *y* axes, respectively, showing a significant negative relationship between these measures in HCS [$r = -0.37$, $P < 10^{-6}$] and a trend negative relationship in SCZ [$r = -0.16$, $P = 0.05$]. Group distributions of each measure are shown on the margins of the scatter plot, highlighting that the mean significant effects for SCZ relative to HCS comprise elevations in GS in association regions and reductions in sensory regions. *d* = Cohen's *d* effect size. Shading represents 95% CI. Also see movement matched analysis in Figure S3, and results without high-pass filtering in Figure S5.

(SCZ-only: $r = -0.68$, $P < 10^{-15}$; HCS only: $r = -0.37$, $P < 10^{-5}$; and all subjects: $r = -0.69$, $P < 10^{-15}$, Fig. 2D).

Of note, we identified a significant relationship between head motion and b_{GS} values in the 2 sets of ROIs. We observed that higher head motion in patients correlated with higher [$r = 0.26$, $P < 0.001$] and lower b_{GS} values [$r = -0.4$, $P < 4 \times 10^{-7}$] in ROIs that were associated with mean elevated and reduced GS localization, respectively. To account for the effect of head motion on our measures, we computed an ANCOVA with head motion as a continuous covariate (measured in % of frames flagged for movement, see Exp. Procedures available in Supplementary Material). Group main effects remained highly significant even after accounting for motion for both ROIs [$F(1,321) = 155.1$, $P < 2 \times 10^{-16}$ for the elevated, and $F(1,321) = 101.9$, $P < 2 \times 10^{-16}$ for the reduced GS localization ROI]. Furthermore, after repeating analyses for a subset of explicitly movement-matched subjects (130 SCZ & 130 HCS) all effects remained highly significant (Figures S2 & S3). Finally, we verified the association versus sensory network-preferential effects via an *a priori* network analysis presented below.

Characterizing Spatial Patterns of GS Beta Changes in SCZ

Voxel-wise results revealed a spatial dissociation between regions of b_{GS} increases and decreases in SCZ, which qualitatively matched association and sensory areas, respectively. To formally quantify the spatial mapping of these shifts, we computed the probability of overlap for these effects with *a priori* defined large-scale functional networks. Here, we defined association and sensory networks using a functional cortical parcellation (Power et al. 2011; Cole et al. 2013). For the "association network" ROI, we combined FPCN, DMN, and the VAN (Fig. 4A). Similarly, we defined the sensory network ROI by combining the somatosensory, auditory, and visual networks (Fig. 4A). "Non-association" and "non-sensory" network ROIs were defined as all cortical gray matter voxels not part of the relevant large-scale network (Fig. 4B,C). Consistent with qualitative observations, voxels showing significantly elevated b_{GS} in SCZ preferentially co-localized to association networks [binomial test for proportions, $P < 0.001$, Fig. 4B,D]. In turn, voxels showing significantly reduced b_{GS} preferentially co-localized to sensory networks [binomial test for proportions, $P < 0.001$, Fig. 4C,D]. A complementary analysis revealed significantly different proportions with respect to spatial coverage of association versus non-association networks by the "mean elevated GS beta" ROI voxels [$P < 0.001$, Fig. 4D]. Similarly, the "mean reduced GS beta" ROI showed significantly different spatial coverage of sensory versus non-sensory networks [$P < 0.001$, Fig. 4D]. Collectively, the overlap analyses indicate that the mean elevated GS beta ROI was predominantly co-localized with association cortices, whereas the mean reduced GS beta ROI was predominantly co-localized with sensory cortices.

Independently Examining GS Representation Shifts in Association versus Sensory Regions

Presented results, in line with recent empirical reports (Yang et al. 2016), suggest network-specific b_{GS} shifts in SCZ. Overlap analyses indicate preferential elevations in b_{GS} in association networks, contrasting with preferential b_{GS} reductions in sensory networks in SCZ. Next, we sought to confirm these effects via an independent *a priori* analysis examining association versus sensory network ROIs. We explicitly examined b_{GS} value differences for SCZ versus HCS across *a priori* functionally defined large-scale networks. Specifically, we averaged voxel-wise b_{GS} across 3 large-scale association networks: FPCN, DMN, and VAN (Fig. 5A), extending our initial focused network characterization (Fig. 4). We found significantly elevated voxel-wise b_{GS} across association regions in SCZ compared with HCS [$t(322) = 3.4$, $P < 0.001$, Cohen's $d = 0.37$] (Fig. 5B,C). Next, we averaged voxel-wise b_{GS} across 3 large-scale sensory networks (Fig. 5A), which revealed significantly reduced voxel-wise b_{GS} across sensory regions in SCZ compared with HCS [$t(322) = 3.8$, $P < 0.0002$, Cohen's $d = 0.42$] (Fig. 5B,C). This effect was confirmed via a *Group* x *Network* interaction (2-way ANOVA for SCZ vs. HCS, association vs. sensory networks [$F(1,323) = 19.7$, $P < 2 \times 10^{-5}$]). In addition, whereas b_{GS} weights are significantly higher in sensory compared with association regions in HCS [$t(163) = 9$, $P < 4 \times 10^{-16}$], the effect size for this network-level difference is reduced in SCZ [$t(160) = 3$, $P = 8 \times 10^{-4}$] (Fig. 5B). We further verified that these independent effects were not driven by amount of head motion or medication dose (Fig. S4A–D). For subjects with available smoking status information, we verified that there were no significant differences between smoker and nonsmoker SCZ patients with respect to reported effects (Fig. S4E,F). Collectively, these empirical effects independently suggest that association and sensory regions show dissociable GS localization changes in SCZ.

Finally, we again verified that the association and sensory b_{GS} effects were quantitatively related (Fig. 5C). As noted above, this analysis revealed a significant negative correlation between mean association and sensory region b_{GS} values across all HCS [$r = -0.37$, $P < 10^{-6}$]. This negative relationship remained significant in SCZ [$r = -0.16$, $P = 0.05$], but the effect size was significantly attenuated [test for difference between correlation coefficients: $z = -2.03$, $P = 0.042$, 2-tailed]. Collectively, these results suggest that the pattern of b_{GS} changes in SCZ may relate to an overall loss of "differentiation" in association versus sensory networks with respect to GS representation.

Of note, some studies (Mueller et al. 2013) have reported greater inter-subject variability in association regions (compared with non-association regions) with respect to functional connectivity. We were thus motivated to examine whether a nonfunctional connectivity measure, such as voxel-wise GS beta weight, might also show greater variability in the association regions. We formally tested this via homogeneity of variance tests, using Bartlett's test and the Fligner–Killeen test. The null hypothesis in this case may be stated as: Let A = the mean voxel-wise GS beta value in the association cortex for a subject; B = the mean voxel-wise GS beta value in the sensory cortex for a subject. The null hypothesis is that the distributions of A and B across subjects have the same variance. This hypothesis was rejected in the healthy subjects group [Bartlett's K-squared = 8.8, $P = 0.003$, df = 1; Fligner–Killeen chi-squared = 6.4, $P = 0.01$, df = 1], with mean association GS beta weight per subject being more variable than the mean sensory GS beta weight per subject, as one might expect if there is overall more variability between individuals in the association regions. Interestingly, the null hypothesis was not rejected for the SCZ group [Bartlett's K-squared = 2.3, $P = 0.13$, df = 1; Fligner–Killeen chi-squared = 2.4, $P = 0.12$, df = 1], again consistent with the idea of less "differentiation" between the association and sensory networks in SCZ.

Discussion

The brain-wide average of all time-varying BOLD signals (i.e. GS) will resemble signal from every part of the brain. However, how much a given area resembles the GS can vary widely. Motivated by recent work suggesting altered GS in SCZ (Yang et al. 2014), we found a complex pattern of increased GS representation in association cortices, but reduced GS representation in sensory-motor cortices. These results replicated across 2 large, independent samples. Across samples, we showed that the 2 alterations are functionally related. Furthermore, findings suggest that GS is represented more strongly in sensory than association regions in healthy subjects. We found that sensory versus association GS representation was strongly anti-correlated in HCS, however this relationship was significantly attenuated in SCZ.

Characterizing GS Topography in Healthy Individuals

While the principal objective of this study was to characterize GS topography shifts in SCZ, the issue of GS topography in healthy individuals has received little quantitative attention in the literature. Seminal work on this topic indeed showed a generally positive correlation between the GS and voxel-wise BOLD

signals in the brain's gray matter (Aguirre et al. 1997; Zarahn et al. 1997; Fox et al. 2009). Yet, an important knowledge gap remained regarding potential network-by-network differences in the distribution of the GS in healthy adults. As noted, we predicted a distinct pattern of GS topography across sensory and association networks given their distinct computational roles in processing time-locked incoming external stimuli versus internal maintenance and representation of parallel information, respectively. As an initial demonstration that voxel-wise GS contributions are indeed nonuniform, we formally quantified GS topography using beta coefficients obtained from a multiple regression. This approach accounts for contributions of GS to the voxel-wise signal along with contributions of multiple nuisance regressors simultaneously, with the GS beta coefficient yielding a quantitative measure of voxel-wise GS contribution. As hypothesized, we found a strong difference in GS representations across *a priori* defined association versus sensory networks (Power et al. 2011), potentially highlighting an intriguing mathematical consequence of the differing computational tasks these networks are specialized to accomplish. However, it remains possible that these dissociable contributions reflect a spatially preferential yet pervasive noise component (e.g. breathing) (Golestani et al. 2015), rather than a true underlying distribution of neuronal signals. Future experimental work that explicitly dissociates physiological and neuronal artifact will be needed to address the underlying mechanisms of this nonuniform GS topography. Nevertheless, it is vital to characterize if this observed GS topography may be altered in severe mental illnesses such as SCZ—a central objective of this study. In turn, such alterations may inform strategies for development of pharmacotherapies, guided by insights from neuroimaging.

Localization of Widespread BOLD Signal Disruption in SCZ

Accumulating evidence from SCZ studies implicates deficits in brain regions responsible for higher-order cognition (Pearlson et al. 1996; Ross and Pearlson 1996; Cannon et al. 2002), with well-established disruptions in executive and working memory functions performed by the frontoparietal networks (Goldman-Rakic 1991; Weinberger et al. 1991; Carter et al. 1998; Barch and Ceaser 2012; Cole et al. 2014). In parallel, different (and perhaps less severe) abnormalities are observed in sensory regions (Woodward et al. 2012; Anticevic et al. 2014; Yang et al. 2014; Yang et al. 2016). This study provides a novel insight into findings implicating sensory versus association regions in SCZ. Put differently, the same pathological process can potentially produce different effects across brain regions that exhibit distinct neurophysiological properties. In healthy subjects, we observed that sensory region BOLD signals showed higher GS resemblance, whereas association areas showed lower GS resemblance. In SCZ, this distinction was shifted whereby association areas resembled the GS more strongly, but sensory areas resembled the GS less, relative to HCS. This bi-directional shift in GS representations could occur through a pathological process that "blurs" the distinction between association and sensory areas, effectively "homogenizing" cortical computations. This would, on average, yield GS elevations in association regions and reductions in sensory regions, as observed in the current study. In the next section, we consider potential neuropathological mechanisms in SCZ that could disrupt patients' ability to (1) broadly integrate sensory information—leading to reduced GS in sensory-motor areas, and (2) maintain independent information representations in association areas—leading to impairments in higher-order cognitive control functions, which may be reflected in increased contribution to GS from association areas.

Understanding Mechanisms of Network-Level Cortical Disruptions in SCZ

As noted, identified cortical GS representation shifts in SCZ follow a functional dissociation between association and sensory cortices. These effects are qualitatively in line with findings observed in corresponding thalamo-cortical circuits (Marenco et al. 2012; Woodward et al. 2012; Anticevic et al. 2014). An open question for future investigation is the directionality of the disturbance in GS representation. Can the pattern of GS shifts be linked to a network-specific pathology, or does it involve a dynamical disturbance across inter-connected systems that makes directionality less central (Loh et al. 2007)?

Several studies suggest association network alterations identified via neuroimaging in SCZ may arise from a localized dysfunction (Lewis 2000; Hashimoto et al. 2003; Kolluri et al. 2005). Notably, the PFC is involved in gating information flow within the brain, and can exert inhibitory top-down control over thalamic nuclei through projections via the basal ganglia (Haber and McFarland 2001). In contrast, sensory regions are considered a source of drive onto the thalamus. Within this framework, we could hypothesize a "primary" association network disruption impacting GS representations as well corresponding thalamo-cortical circuits. In turn, this could lead to "secondary" disruptions, altering the balance of activity amongst thalamic nuclei, leading to concurrent (but not primary) global effects in sensory networks. Such a pattern of thalamo-cortical disruptions is consistent with prior reports (Marenco et al. 2012; Woodward et al. 2012; Anticevic et al. 2014).

Conversely, other SCZ neuropathology frameworks favor a more spatially distributed primary pathology across cortical circuits. Growing evidence from preclinical, pharmacological, and postmortem clinical studies implicates disrupted E/I balance across cortical microcircuits in SCZ (Marin 2012). This could reflect changes in a number of candidate neurotransmitter systems, involving glutamate (Krystal et al. 2003; Macdonald and Chafee 2006), GABA (Lewis et al. 2005), and dopamine pathways (Laruelle et al. 2003). Such changes potentially impact neural development, causing global impairments in integration/segregation of neural processing, as is suggested by studies of SCZ and their siblings (Repovs et al. 2011; Repovs and Barch 2012). How can we reconcile these hypothesized cellular-level disruptions with observed network-level BOLD abnormalities? Our prior computational modeling work identified altered E/I balance in cortical circuits as a key mechanism for disrupted long-range interactions between cortical areas (Anticevic, Gancsos et al. 2012), with preferential impact upon association networks at rest (Yang et al. 2016). This work offers a potential mechanism for the observed "blurring" between association and sensory networks with respect to GS localization. Here we show that the tightly anti-correlated relationship between these networks becomes attenuated in SCZ relative to HCS. This reduction in anti-correlated patterns between association and sensory GS representations may relate to the same disinhibition-mediated mechanism that reduces anti-correlations between task-positive and task-negative networks in SCZ (Anticevic, Gancsos et al. 2012). Furthermore, the observed opposing effects in association versus sensory networks may relate to preexisting intrinsic differences between these networks that alter the impact of E/I

imbalance on these networks (Yang et al. 2016). In summary, these cortical models of global E/I imbalance suggest that disrupted long-range anti-correlations (Anticevic, Gancsos et al. 2012) and network-dependent pathological changes (Yang et al. 2016) might de-stabilize cortical information flow in ways observed presently: manifesting as altered GS representations for sensory versus association networks in SCZ. Future pharmacological and animal studies will be needed close the gaps between these emerging cellular hypotheses and system-level observations in SCZ.

Implications for Disrupted Cortical Information Flow in SCZ

Disruptions in E/I balance in SCZ may profoundly affect large-scale cortical function (Anticevic et al. 2013; Uhlhaas 2013). Indeed, prior computational studies show that E/I imbalance can alter functional connectivity and variance of BOLD signals across cortex (Yang et al. 2014, 2016). However, clinical studies of SCZ and HCS show that between-group differences across both measures are sensitive to GSR (Yang et al. 2014). This indicates that group differences may need to be considered in context of potential group-level changes in the GS representation itself, even if they partially reflect nuisance signal. Here, we quantified group-level GS shifts using 2 well-powered independent samples. Across samples, SCZ patients showed significantly reduced GS representation in sensory networks. Concurrently, we observed increased GS representation in association networks. Overall, network-level differences in GS representation were significantly reduced in SCZ. In contrast, HCS showed significantly greater GS localization in sensory compared with association networks. As noted, this complex spatial shift in cortical GS representation provides whole-brain evidence that, in SCZ, GS localizations may not differentiate well between the association and sensory cortices, possibly reflective of a "blurring" between sensory-association signals flowing through the brain.

Of note, reported effects show that these hyper- and hypo-localizations of GS are highly related: HCS with lower voxel-wise GS beta values in association networks exhibited increased GS beta values in sensory networks. In SCZ, this anti-correlated relationship was significantly reduced. This is an important consideration for treatments designed to restore neural function. For instance, interventions with regional selectivity, like low-frequency transcranial magnetic stimulation, might treat some symptoms (Hoffman et al. 1999; Fox et al. 2012; Demirtas-Tatlidede et al. 2013). However, such interventions may disrupt tightly anti-correlated processes occurring in different large-scale neural networks by further de-coupling such systems. Alternatively, a careful characterization of internetwork dynamics may inform the refinement of future interventions toward re-establishing a healthy functional regime across networks. These are speculative possibilities, but prospective investigations incorporating detailed computational models of large-scale cortical network interactions may deepen our intuition for such complex dynamics (Yang et al. 2016).

Relating Findings to Diagnosis, Treatment, and Active Symptoms

As noted above, SCZ subjects differed from HCS in 3 key measures with respect to GS beta weights computed from their rs-fMRI data (also see Fig. 5): (1) SCZ showed significantly increased mean association region b_{GS} values relative to HCS, (2) SCZ showed significantly reduced mean sensory region b_{GS} values relative to HCS, and (3) network-level differences (association vs. sensory) were substantially reduced in SCZ. We cannot rule out the possibility that these diagnosis-related group-level differences could relate to treatment effects, since all SCZ patients were receiving medication, however none of the effects were significantly related to medication dosage (Figure S4). We did not discover any significant relationships between our findings and active symptoms obtained from patient PANSS scores.

Considering Inter-Subject Variability in Association Regions

Prior studies in healthy subjects (Mueller et al. 2013) have observed greater inter-subject variability in association regions (compared with non-association regions) with respect to functional connectivity. We report a similar finding of increased inter-subject variability in association regions in healthy subjects, with respect to a different measure: network-averaged voxel-wise GS beta weights, which impact functional connectivity measures but are not themselves measures of pair-wise connectivity between regions in the sense that a Pearson's correlation in a connectivity matrix would be. This finding motivates several questions for potential future study: what mechanism, if any, could plausibly link increased association region variability in functional connectivity to the same increased variability in network-averaged GS beta weights? Why is this elevation in between-subject variability in mean association b_{GS} values (compared with mean sensory b_{GS} values) seemingly absent in the SCZ cohort? Finally, if the GS topography is nonuniform in healthy subjects and differently distributed in SCZ, could GSR during preprocessing affect signals in some brain regions more than others?

Limitations

Some important limitations need to be considered. The combined SCZ sample, although large and well characterized, was associated with comorbid history of drug/alcohol abuse/dependence to provide more generalizability to patients typically encountered in the population. In addition, it is important to establish if treatments can attenuate observed effects. We could not address this question in our study. While present control analyses argue against medication confounds, medication remains a vital consideration for future studies. Notably, patients were medicated. Although medication dose did not alter effects statistically, long-term medication might impact patterns of network-level cortical activity independently of the illness. Thus, it will be critical to replicate findings across unmedicated, prodromal, at-risk, or first-degree relatives of patients. Because of correlational measures, it is unclear whether changes reflect the cause or the consequence of the illness, which may be associated with dynamical circuit alterations over time. To disambiguate these causal possibilities, it will be important to determine if observed disturbances relate to illness duration, number of psychotic episodes, and occur in at-risk populations. We observed no significant relationships between head motion, medication levels, smoking and GS beta weights in association and sensory networks (Figure S4).

A final set of limitations relates to use of single-band (SB) BOLD acquisition and complementary volume-based registration and processing methods that limit spatial and temporal resolution (Glasser et al. 2013; Robinson et al. 2014). This leads to extensive mixing across tissue types and brain areas and makes the spatial patterns interpretable only at large scales

(e.g. the broad sensory vs. cognitive network distinctions). Thus, these findings should be replicated and characterized via high spatial resolution functional multi-band (MB) BOLD data processed using cutting-edge surface-based registration (Glasser et al. 2013; Robinson et al. 2014). Also, future studies using faster temporal resolution MB data will permit more sophisticated de-noising strategies (e.g. data-driven approaches like ICA+FIX), which will facilitate better detection and elimination of motion and physiological artifact. Relatedly, this study could not separate sources of GS gray matter variance. For instance, several physiological parameters explain a substantial fraction of the GS. These include differences in end tidal pCO2 concentration, breathing rate/depth, and heart rate variations (Golestani et al. 2015). Put differently, due to the relatively low temporal resolution of our data, it is likely that heart beat effects are aliased into the BOLD frequency range. This is an issue commonly affecting fMRI studies with slower TRs (Cordes et al. 2014). As noted, this may be addressable via faster TR sampling available using multiband acquisition that permits sub-second TRs. Therefore, our present data cannot be used to address the question of whether the observed GS topography differences arise from neurological versus physiological sources. This is an important consideration, as we do not definitively know to what extent differences in GS magnitude, or spatial distribution, reflect physiological or neural differences between SCZ and HCS. Addressing this issue will critically inform further refinement of reported effects and their viability as a disease marker.

Despite these caveats, this study involved a well-powered large sample collected via "legacy" SB approaches, which permits a broad neuroanatomical and functional analysis of the GS pattern in SCZ. Furthermore, our study replicated effects across 2 samples from different sites, making it less likely that effects were driven by systematically consistent physiological artifacts across both samples. Another promising aspect of our findings is that they are present bilaterally and dissociate across association and sensory regions, in contrast to findings in studies evaluating physiological artifacts in BOLD signals across the brain (Cordes et al. 2014; Jennings et al. 2016). These studies largely seem to find effects in both association and sensory regions without showing dissociation between them (Cordes et al. 2014). Nevertheless, a more careful spatial and temporal characterization of this effect, along with simultaneous monitoring of heart beat and respiration, would be vital for future work.

Conclusion

This study is the first to quantify, from a network-by-network perspective, the spatially varying component of GS representation across the whole brain in healthy subjects and patients with SCZ. This examination uncovered a strikingly anti-correlated relationship in GS representation in association versus sensory networks across healthy subjects, with association regions showing a significantly smaller GS component than did sensory regions. Further, we systematically characterized, in a data-driven and anatomically based fashion, spatial shifts in GS representation in SCZ—a severe psychiatric illness associated with brain-wide alterations. We concurrently observed robust reductions and increases in sensory and association network GS representations in SCZ, respectively. Results suggest strong and functionally related GS localization disturbances across these large-scale networks. These GS disturbances were not strongly related to severity of clinical symptoms, suggesting that they may be an invariant "trait-like" feature of this illness. Collectively, these effects suggest that disrupted GS localization across networks may serve as a robust clinical marker and might reflect a final common pathway of neural system disturbances in SCZ reflecting "blurred" neural information flow.

Supplementary Material

Supplementary material can be found at: http://www.cercor.oxfordjournals.org/.

Funding

National Institutes of Health (grant DP50D012109-03 to A.A., PI (principal investigator), and grant T32GM 007205 to G.J.Y.), and MH43775, MH077945, and MH074797 (to G.D.P., PI); National Institute on Alcohol Abuse and Alcoholism (grant 2P50AA012870-11 to J.H.K., PI), and National Institute of Mental Health (grant F30 MH107149 to G.J.Y.).

Notes

We would like to acknowledge Dr. Jonathan Power for providing helpful feedback on the manuscript. *Conflict of Interest*: None declared.

References

Aguirre GK, Zarahn E, D'Esposito M. 1997. Empirical analyses of BOLD fMRI statistics. II. Spatially smoothed data collected under null-hypothesis and experimental conditions. Neuroimage. 5:199–212.

Akbarian S, Sucher NJ, Bradley D, Tafazzoli A, Trinh D, Hetrick WP, Potkin SG, Sandman CA, Bunney WEJr, Jones EG. 1996. Selective alterations in gene expression for NMDA receptor subunits in prefrontal cortex of schizophrenics. J Neurosci. 16:19–30.

Andreasen NC, Pressler M, Nopoulos P, Miller D, Ho B-C. 2010. Antipsychotic dose equivalents and dose-years: a standardized method for comparing exposure to different drugs. Biol Psychiatry. 67:255–262.

Anticevic A, Brumbaugh MS, Winkler AM, Lombardo LE, Barrett J, Corlett PR, Kober H, Gruber J, Repovs G, Cole MW, et al. 2012. Global prefrontal and fronto-amygdala dysconnectivity in bipolar i disorder with psychosis history. Biol Psychiatry. 73:565–573.

Anticevic A, Cole MW, Repovs G, Murray JD, Brumbaugh MS, Winkler AM, Savic A, Krystal JH, Pearlson GD, Glahn DC. 2014. Characterizing thalamo-cortical disturbances in schizophrenia and bipolar illness. Cereb Cortex. 24:3116–3130.

Anticevic A, Cole MW, Repovs G, Savic A, Driesen NR, Yang G, Cho YT, Murray JD, Glahn DC, Wang X-J, et al. 2013. Connectivity, pharmacology, and computation: toward a mechanistic understanding of neural system dysfunction in schizophrenia. Front Psychiatry. 4:1–21.

Anticevic A, Gancsos M, Murray JD, Repovs G, Driesen NR, Ennis DJ, Niciu MJ, Morgan PT, Surti TS, Bloch MH, et al. 2012. NMDA receptor function in large-scale anti-correlated neural systems with implications for cognition and schizophrenia. Proc Natl Acad Sci USA. 109:16720–16725.

Baker JT, Holmes AJ, Masters GA, Yeo BT, Krienen F, Buckner RL, Ongur D. 2014. Disruption of cortical association networks in schizophrenia and psychotic bipolar disorder. JAMA Psychiatry. 71:109–118.

Barch DM, Ceaser A. 2012. Cognition in schizophrenia: core psychological and neural mechanisms. Trends Cogn Sci. 16:27–34.

Berenbaum H, Oltmanns TF. 1992. Emotional experience and expression in schizophrenia and depression. J Abnorm Psychol. 101:37–44.

Calderone DJ, Martinez A, Zemon V, Hoptman MJ, Hu G, Watkins JE, Javitt DC, Butler PD. 2013. Comparison of psychophysical, electrophysiological, and fMRI assessment of visual contrast responses in patients with schizophrenia. Neuroimage. 67:153–162.

Cannon TD, Thompson PM, van Erp TG, Toga AW, Poutanen VP, Huttunen M, Lonnqvist J, Standerskjold-Nordenstam CG, Narr KL, Khaledy M, et al. 2002. Cortex mapping reveals regionally specific patterns of genetic and disease-specific gray-matter deficits in twins discordant for schizophrenia. Proc Natl Acad Sci USA. 99:3228–3233.

Carter CS, Perlstein W, Ganguli R, Brar J, Mintun M, Cohen JD. 1998. Functional hypofrontality and working memory dysfunction in schizophrenia. Am J Psychiatry. 155:1285–1287.

Cohen AL, Fair DA, Dosenbach NU, Miezin FM, Dierker D, Van Essen DC, Schlaggar BL, Petersen SE. 2008. Defining functional areas in individual human brains using resting functional connectivity MRI. Neuroimage. 41:45–57.

Cole MW, Anticevic A, Repovs G, Barch DM. 2011. Variable global dysconnectivity and individual differences in schizophrenia. Biol Psychiatry. 70:43–50.

Cole MW, Repovs G, Anticevic A. 2014. The frontoparietal control system: a central role in mental health. Neuroscientist. 20:652–664.

Cole MW, Reynolds JR, Power JD, Repovs G, Anticevic A, Braver TS. 2013. Multi-task connectivity reveals flexible hubs for adaptive task control. Nat Neurosci. 16:1348–1355.

Cordes D, Nandy RR, Schafer S, Wager TD. 2014. Characterization and reduction of cardiac- and respiratory-induced noise as a function of the sampling rate (TR) in fMRI. Neuroimage. 89: 314–330.

Demirtas-Tatlidede A, Vahabzadeh-Hagh AM, Pascual-Leone A. 2013. Can noninvasive brain stimulation enhance cognition in neuropsychiatric disorders? Neuropharmacology. 64: 566–578.

Dracheva S, Marras SA, Elhakem SL, Kramer FR, Davis KL, Haroutunian V. 2001. N-methyl-D-aspartic acid receptor expression in the dorsolateral prefrontal cortex of elderly patients with schizophrenia. Am J Psychiatry. 158: 1400–1410.

First MB, Spitzer RL, Miriam G, Williams JBW. 2002.Structured clinical interview for DSM-IV-TR axis I disorders, research version, non-patient edition (SCID-I/NP). New York: Biometrics Research, New York State Psychiatric Institute.

Fox M, Zhang D, Snyder A, Raichle M. 2009. The global signal and observed anticorrelated resting state brain networks. J Neurophysiol. 101:3270–3283.

Fox MD, Buckner RL, White MP, Greicius MD, Pascual-Leone A. 2012. Efficacy of transcranial magnetic stimulation targets for depression is related to intrinsic functional connectivity with the subgenual cingulate. Biol Psychiatry. 72: 595–603.

Glahn DC, Bearden CE, Bowden CL, Soares JC. 2006. Reduced educational attainment in bipolar disorder. J Affect Disord. 92:309–312.

Glantz LA, Lewis DA. 2000. Decreased dendritic spine density on prefrontal cortical pyramidal neurons in schizophrenia. Arch Gen Psychiatry. 57:65–73.

Glasser MF, Sotiropoulos SN, Wilson JA, Coalson TS, Fischl B, Andersson JL, Xu J, Jbabdi S, Webster M, Polimeni JR, et al. Consortium W-MH. 2013. The minimal preprocessing pipelines for the human connectome project. Neuroimage. 80: 105–124

Goldman-Rakic PS. 1991. Prefrontal cortical dysfunction in schizophrenia: the relevance of working memory. In: Carroll BJ, Barrett JE, editors. Psychopathology and the brain. New York: Raven Press, Ltd. p. 1–23.

Goldman-Rakic PS. 1994. Working memory dysfunction in schizophrenia. J Neuropsychiatr. 6:348–357.

Golestani AM, Chang C, Kwinta JB, Khatamian YB, Jean Chen J. 2015. Mapping the end-tidal CO2 response function in the resting-state BOLD fMRI signal: spatial specificity, test-retest reliability and effect of fMRI sampling rate. Neuroimage. 104:266–277.

Gupta CN, Calhoun VD, Rachakonda S, Chen J, Patel V, Liu J, Segall J, Franke B, Zwiers MP, Arias-Vasquez A, et al. 2015. Patterns of gray matter abnormalities in schizophrenia based on an international mega-analysis. Schizophr Bull. 41: 1133–42.

Haber S, McFarland NR. 2001. The place of the thalamus in frontal cortical-basal ganglia circuits. Neuroscientist. 7: 315–324.

Hanlon FM, Houck JM, Pyeatt CJ, Lundy SL, Euler MJ, Weisend MP, Thoma RJ, Bustillo JR, Miller GA, Tesche CD. 2011. Bilateral hippocampal dysfunction in schizophrenia. Neuroimage. 58:1158–1168.

Hashimoto T, Bazmi HH, Mirnics K, Wu Q, Sampson AR, Lewis DA. 2008. Conserved regional patterns of GABA-related transcript expression in the neocortex of subjects with schizophrenia. Am J Psychiatry. 165:479–489.

Hashimoto T, Volk DW, Eggan SM, Mirnics K, Pierri JN, Sun Z, Sampson AR, Lewis DA. 2003. Gene expression deficits in a subclass of GABA neurons in the prefrontal cortex of subjects with schizophrenia. J Neurosci. 23:6315–6326.

Hoffman RE, Boutros NN, Berman RM, Roessler E, Belger A, Krystal JH, Charney DS. 1999. Transcranial magnetic stimulation of left temporoparietal cortex in three patients reporting hallucinated "voices". Biol Psychiatry. 46:130–132.

Hoffman RE, Fernandez T, Pittman B, Hampson M. 2011. Elevated functional connectivity along a corticostriatal loop and the mechanism of auditory/verbal hallucinations in patients with schizophrenia. Biol Psychiatry. 69:407–414.

Jardri R, Deneve S. 2013. Circular inferences in schizophrenia. Brain. 136:3227–3241.

Javitt DC, Strous RD, Grochowski S, Ritter W, Cowan N. 1997. Impaired precision, but normal retention, of auditory sensory ("echoic") memory information in schizophrenia. J Abnorm Psychol. 106:315–324.

Jennings JR, Sheu LK, Kuan DC, Manuck SB, Gianaros PJ. 2016. Resting state connectivity of the medial prefrontal cortex covaries with individual differences in high-frequency heart rate variability. Psychophysiology. 53:444–454.

Johnson MR, Morris NA, Astur RS, Calhoun VD, Mathalon DH, Kiehl KA, Pearlson GD. 2006. A functional magnetic resonance imaging study of working memory abnormalities in schizophrenia. Biol Psychiatry. 60:11–21.

Kay SR, Fiszbein A, Opler LA. 1987. The positive and negative syndrome scale (PANSS) for schizophrenia. Schizophr Bull. 13:261–276.

Kolluri N, Sun Z, Sampson AR, Lewis DA. 2005. Lamina-specific reductions in dendritic spine density in the prefrontal cortex

of subjects with schizophrenia. Am J Psychiatry. 162: 1200–1202.

Krystal JH, D'Souza DC, Gallinat J, Driesen NR, Abi-Dargham A, Petrakis I, Heinz A, Pearlson GD. 2006. The vulnerability to alcohol and substance abuse in individuals diagnosed with schizophrenia. Neurotox Res. 10:235–252.

Krystal JH, D'Souza DC, Mathalon D, Perry E, Belger A, Hoffman R. 2003. NMDA receptor antagonist effects, cortical glutamatergic function, and schizophrenia: toward a paradigm shift in medication development. Psychopharmacology (Berl). 169:215–233.

Laruelle M, Kegeles LS, Abi-Dargham A. 2003. Glutamate, dopamine, and schizophrenia: from pathophysiology to treatment. Ann N Y Acad Sci. 1003:138–158.

Lencz T, Bilder RM, Turkel E, Goldman RS, Robinson D, Kane JM, Lieverman JA. 2003. Impairments in perceptual competency and maintenance on a visual delayed match-to-sample test in first-episode schizophrenia. Arch Gen Psychiatry. 60: 238–243.

Lewis DA. 2000. Is there a neuropathology of schizophrenia? Recent findings converge on altered thalamic-prefrontal cortical connectivity. Neuroscientist. 6:208–218.

Lewis DA, Hashimoto T, Volk DW. 2005. Cortical inhibitory neurons and schizophrenia. Nat Rev Neurosci. 6:312–324.

Lezak MD. 1995. Neuropsychological assessment. New York: Oxford University Press.

Loh M, Rolls ET, Deco G. 2007. A dynamical systems hypothesis of schizophrenia. PLoS Comput Biol. 3:e228.

Lowe MJ. 2012. The emergence of doing "nothing" as a viable paradigm design. Neuroimage. 62:1146–1151.

Macdonald AW, Chafee MV. 2006. Translational and developmental perspective on N-methyl-D-aspartate synaptic deficits in schizophrenia. Dev Psychopathol. 18:853–876.

Maldonado-Aviles JG, Curley AA, Hashimoto T, Morrow AL, Ramsey AJ, O'Donnell P, Volk DW, Lewis DA. 2009. Altered markers of tonic inhibition in the dorsolateral prefrontal cortex of subjects with schizophrenia. Am J Psychiatry. 166: 450–459.

Marenco S, Stein JL, Savostyanova AA, Sambataro F, Tan HY, Goldman AL, Verchinski BA, Barnett AS, Dickinson D, Apud JA, et al. 2012. Investigation of anatomical thalamo-cortical connectivity and FMRI activation in schizophrenia. Neuropsychopharmacology. 37:499–507.

Marin O. 2012. Interneuron dysfunction in psychiatric disorders. Nat Rev Neurosci. 13:107–120.

Marsman A, Mandl RC, Klomp DW, Bohlken MM, Boer VO, Andreychenko A, Cahn W, Kahn RS, Luijten PR, Hulshoff Pol HE. 2014. GABA and glutamate in schizophrenia: a 7 T (1)H-MRS study. Neuroimage Clin. 6:398–407.

Marsman A, van den Heuvel MP, Klomp DWJ, Kahn RS, Luijten PR, Hulshoff Pol HE. 2013. Glutamate in schizophrenia: a focused review and meta-analysis of 1H-MRS studies. Schizophr Bull. 39:120–129

Mayer AR, Ruhl D, Merideth F, Ling J, Hanlon FM, Bustillo J, Cañive J. 2012. Functional imaging of the hemodynamic sensory gating response in schizophrenia. Hum Brain Mapp. 34: 2302–2312.

Mueller S, Wang D, Fox MD, Yeo BT, Sepulcre J, Sabuncu MR, Shafee R, Lu J, Liu H. 2013. Individual variability in functional connectivity architecture of the human brain. Neuron. 77:586–595.

Pearlson GD, Petty RG, Ross CA, Tien AY. 1996. Schizophrenia: a disease of heteromodal association cortex? Neuropsychopharmacology. 14:1–17.

Poels EM, Kegeles LS, Kantrowitz JT, Javitt DC, Lieberman JA, Abi-Dargham A, Girgis RR. 2014. Glutamatergic abnormalities in schizophrenia: a review of proton MRS findings. Schizophr Res. 152:325–332.

Power JD, Cohen AL, Nelson SM, Wig GS, Barnes KA, Church JA, Vogel AC, Laumann TO, Miezin FM, Schlaggar BL, et al. 2011. Functional network organization of the human brain. Neuron. 72:665–678.

Power JD, Mitra A, Laumann TO, Snyder AZ, Schlaggar BL, Petersen SE. 2014. Methods to detect, characterize, and remove motion artifact in resting state fMRI. Neuroimage. 84:320–341.

Radhu N, Garcia Dominguez L, Farzan F, Richter MA, Semeralul MO, Chen R, Fitzgerald PB, Daskalakis ZJ. 2015. Evidence for inhibitory deficits in the prefrontal cortex in schizophrenia. Brain. 138:483–497.

Repovs G, Barch DM. 2012. Working memory related brain network connectivity in individuals with schizophrenia and their siblings. Front Hum Neurosci. 6:1–15.

Repovs G, Csernansky JG, Barch DM. 2011. Brain network connectivity in individuals with schizophrenia and their siblings. Biol Psychiatry. 15:967–973.

Robinson EC, Jbabdi S, Glasser MF, Andersson J, Burgess GC, Harms MP, Smith SM, Van Essen DC, Jenkinson M. 2014. MSM: a new flexible framework for Multimodal Surface Matching. Neuroimage. 100:414–426.

Ross CA, Pearlson GD. 1996. Schizophrenia, the heteromodal association neocortex and development: potential for a neurogenetic approach. Trends Neurosci. 19:171–176.

Saad ZS, Gotts SJ, Murphy K, Chen G, Jo HJ, Martin A, Cox RW. 2012. Trouble at rest: how correlation patterns and group differences become distorted after global signal regression. Brain Connect. 2:25–32.

Schobel SA, Chaudhury NH, Khan UA, Paniagua B, Styner MA, Asllani I, Inbar BP, Corcoran CM, Lieberman JA, Moore H, et al. 2013. Imaging patients with psychosis and a mouse model establishes a spreading pattern of hippocampal dysfunction and implicates glutamate as a driver. Neuron. 10:81–93.

Schölvinck ML, Maier A, Ye FQ, Duyn JH, Leopold DA. 2010. Neural basis of global resting-state fMRI activity. Proc Natl Acad Sci USA. 107:10238–10243.

Spreen O, Strauss E. 1998.A compendium of neuropsychological tests: administration, norms, and commentary. New York: Oxford University Press.

Stephan KE, Friston KJ, Frith CD. 2009. Dysconnection in schizophrenia: from abnormal synaptic plasticity to failures of self-monitoring. Schizophr Bull. 35:509–527.

Stephan KE, Penny WD, Daunizeau J, Moran RJ, Friston KJ. 2009. Bayesian model selection for group studies. Neuroimage. 46: 1004–1017.

Taylor SF, Tso IF. 2015. GABA abnormalities in schizophrenia: a methodological review of in vivo studies. Schizophr Res. 167:84–90.

Tek C, Gold J, Blaxton T, Wilk C, McMahon RP, Buchanan RW. 2002. Visual perceptual and working memory impairments in schizophrenia. Arch Gen Psychiatry. 59:146–153.

Uhlhaas PJ. 2013. Dysconnectivity, large-scale networks and neuronal dynamics in schizophrenia. Curr Opin Neurobiol. 23:283–290.

Vercammen A, Knegtering H, den Boer JA, Liemburg EJ, Aleman A. 2010. Auditory hallucinations in schizophrenia are associated with reduced functional connectivity of the temporo-parietal area. Biol Psychiatry. 67: 912–918.

Weinberger DR, Berman KF, Daniel DG. 1991. Prefrontal cortex dysfunction in schizophrenia. In: Levin HS, Eisenberg HM, Benton AL, editors. Frontal lobe function and dysfunction. New York: Oxford University Press. p. 276–285.

Welsh RC, Chen AC, Taylor SF. 2010. Low-frequency BOLD fluctuations demonstrate altered thalamocortical connectivity in schizophrenia. Schizophr Bull. 36:713–722.

Whitfield-Gabrieli S, Thermenos H, Milanovic S, Tsuang M, Faraone S, McCarley R, Shenton M, Green A, Nieto-Castanon A, Laviolette P, et al. 2009. Hyperactivity and hyperconnectivity of the default network in schizophrenia and in first-degree relatives of persons with schizophrenia. Proc Natl Acad Sci USA. 106:1279–1284.

Woodward ND, Karbasforoushan H, Heckers S. 2012. Thalamocortical dysconnectivity in schizophrenia. Am J Psychiatry. 169:1092–1099.

Yang GJ, Murray JD, Repovs G, Cole MW, Savic A, Glasser MF, Pittenger C, Krystal JH, Wang XJ, Pearlson GD, et al. 2014. Altered global brain signal in schizophrenia. Proc Natl Acad Sci USA. 111:7438–7443.

Yang GJ, Murray JD, Wang XJ, Glahn DC, Pearlson GD, Repovs G, Krystal JH, Anticevic A. 2016. Functional hierarchy underlies preferential connectivity disturbances in schizophrenia. Proc Natl Acad Sci USA. 113:E219–228.

Zarahn E, Aguirre GK, D'Esposito M. 1997. Empirical analyses of BOLD fMRI statistics. I. Spatially unsmoothed data collected under null-hypothesis conditions. Neuroimage. 5:179–197.